IEEE Access
Multidisciplinary ⋮ Rapid Review ⋮ Open Access Journal

Received January 21, 2022, accepted March 21, 2022, date of publication April 7, 2022, date of current version April 19, 2022.

Digital Object Identifier 10.1109/ACCESS.2022.3165553

Comprehensive Overview on HVDC Converter Transformer Design: Additional Discussions to the IEC/IEEE 60076-57-129 Standard

MARCOS V. CZERNORUCKI[1], MAURICIO B. C. SALLES[1], (Member, IEEE), EDUARDO C. M. COSTA[1], (Member, IEEE), ANDRE S. MELO[1], AND LUIGI PIEGARI[2], (Senior Member, IEEE)

[1]Laboratory of Advanced Electric Grids (LGRID), Department of Electrical Energy and Automation Engineering, University of São Paulo, São Paulo 05508-010, Brazil

[2]Department of Electronics, Information and Bioengineering, Politecnico di Milano, 20133 Milan, Italy

Corresponding author: Marcos V. Czernorucki (marcosczcki@alumni.usp.br)

This work was supported in part by the Coordenação de Aperfeiçoamento de Pessoal de Nível Superior (CAPES), Brazil, under Grant 001; and in part by Hitachi Energy for the use of the mentioned figures.

ABSTRACT HVDC has been chosen as an economical and technical solution for power transmission through long distances, asynchronous interconnections and long submarine cables crossing. Despite DC transmission benefits to power systems, the converters non-linearity produces undesirable effects to the converter transformer in service, mainly listed in the technical standard IEC/IEEE 60076-57-129. However, additional discussions and complementary information can be found in a plurality of references, which are brought in the article under a comprehensive overview perspective. Some design solutions deal with these effects increasing the technical margins, which have direct influence on manufacturing costs and transformer reliability and availability levels. This article goes through the main topics pointed by the standard and the references, investigating their consequences in the converter transformer operation, in order to provide a comprehensive tutorial on design solutions and considerations to deal with those undesirable effects.

INDEX TERMS HVDC, transformer, standard, design.

I. INTRODUCTION

The HVDC system technology became commercially and practical feasible with the advent of the mercury-arc valves in the 1950's, developed to solid-state thyristors in late 1960's and introduced new technologies, allowing DC transmission implementation on a wider number of applications in the late of 1990's [1]. It has been considered a technical and economical solution for bulk energy transmission in long distances, to interconnect asynchronous systems and provide power delivery through long submarine cables crossing. The global interest in the HVDC system solutions is evident by the number of projects implemented along the latest years [2].

Nowadays, renewable energy generation represents an important share of the global energetic matrix, as a reliable, environmental, and economical solution, contributing in a strategic way to the global carbon generation drop policies [3]. HVDC technology can integrate different renewable energy sources, promoting enough reliability and power quality for energy transportation, even under uncertainty wind flow and sunshine intensity [4]. It also provides a higher system efficiency when compared to an equivalent high-voltage AC system [5]–[7], connecting energy generation plants between different regions, countries or even continents. Thus, HVDC increases the electricity market relations [8] and helps to strength networks short-circuit power, increasing reliability and energy availability, under a smart grid prospective [4], [9]. In this context, some worldwide projects can be mentioned, such as BritNed project connecting Great Britain to the Netherlands, Fenno-Skan connecting Finland to Sweden [10], or EuroAsia and EuroAfrica interconnections between Israel-Greece and Egypt-Greece respectively.

Some reasons make HVDC more competitive than HVAC for power transmission through very long distances. The reduced number of conductors results in less overhead line material, decreases the environmental impact and the terrain expropriation costs [11], reflecting in more than 50% right-of-way shrinkage, illustrated in Fig. 1. The costs are

The associate editor coordinating the review of this manuscript and approving it for publication was Ali Raza.

further reduced (around 25 to 35%), because HVDC does not require reactive compensation along the overhead lines, and underground or submarine cables. Furthermore, the losses in the power transmission are mitigated, between 30 to 40% [12], due to conductors' skin effect elimination [13]. The Fig. 2 compares the costs to transmit 18000MW over 2000 km under some stipulated percentage of line losses.

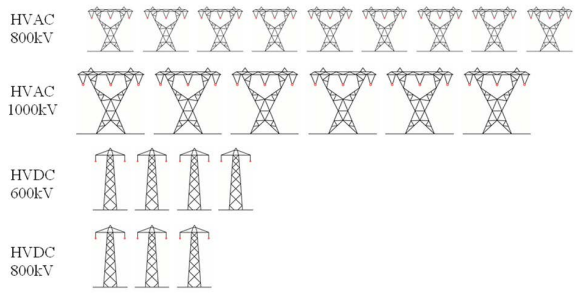

FIGURE 1. Different configurations to transport 18GW over a 2000km distance, adopted from [16].

The HVDC systems represent an efficient solution for interconnecting asynchronous systems, since DC installation is a buffer, isolating the systems electrically [14]. It can also connect 50Hz and 60Hz electrical system, e.g., the Itaipu link between Paraguay and Brazil, which transmits 6300MW over 800km by a ±600kVdc line [15]. Finally, DC links can operate synchronized with AC systems, improving the power flow control, avoiding cascade failures and blackouts [16].

The Fig. 3 illustrates the break-even point where an HVDC installation becomes commercially competitive. The break-even distance differs between overhead transmission lines and underground/submarine cables due to material cost base [17]. The HVDC system main costs refer to the converter station, including the valve hall, smoothing reactor, transformers, and the converter valves, and are not essentially related to the overhead lines. The HVAC initial costs are lower, increasing while the transmission reaches longer distances, due to the reactive compensation, represented by the dashed lines [18].

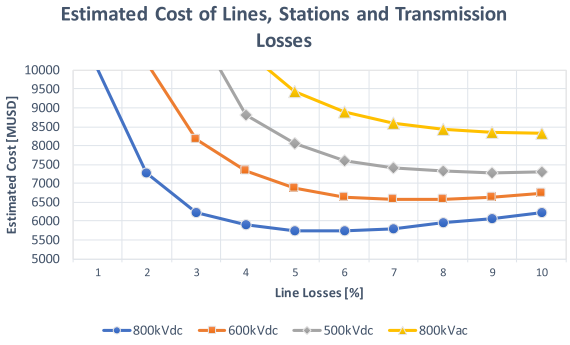

FIGURE 2. Cost comparison to transport 18GW over 2000 km distance, adopted from [16].

The total system cost is a combination of the terminal installation and the energy losses, represented by the continuous lines in Fig. 3 [15].

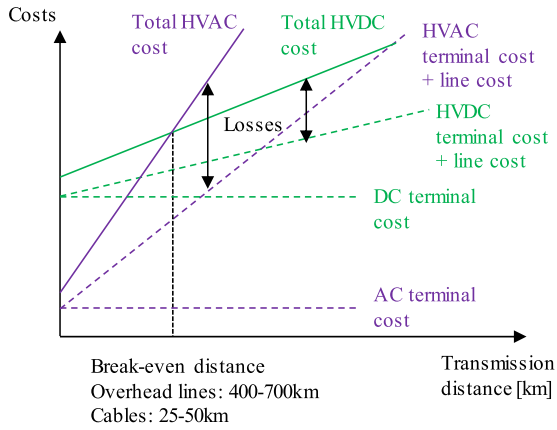

FIGURE 3. Comparative cost between HVAC and HVDC systems as a function of the line length, adopted from [15] and [19].

II. HVDC TECHNOLOGY

A. WORLDWIDE APPLICATION

The AC technology is being successfully applied in the power generation, transmission, and distribution systems worldwide. Nevertheless, it has technical and economical limitations on implementation and operation, that make the DC transmission a realistic and, often, an even unique alternative [20].

The greatest HVDC installations are located mainly in China and India. In the references [21]–[26] the reader can find HVDC links worldwide, listed by the commissioning date, country of installation, transmission line length, DC system voltage, transmission power and DC current. The references [27]–[33] provide an overview on the HVDC projects in operation, categorizing reliability, performance, energy availability, energy utilization, forced and scheduled outages and other data taken from different utilities along the years.

Nowadays, there are two basic converter topologies commonly applied: the line-commutated Current Source Converter (LCC or CSC) and the self-commutated Voltage Source Converter (VSC) [34].

B. HVDC SYSTEM TOPOLOGIES

1) LINE-COMMUTATED CURRENT SOURCE CONVERTER

The conventional line-commutated LCC (Figs. 4a and 4b) is built using a six-pulse or Graetz bridge. Commonly, two six-pulse bridges are connected in series, resulting in a twelve-pulse bridge in cascade. One transformer is connected to each 6-pulse bridge, having different phase displacement in the valve terminal. One is built in a delta connection and the other is wye connected. A thirty-degree displacement is applied to the AC voltage source, establishing a distinct thyristor firing sequence within the period. This combined operation does not eliminate the fifth and seventh current harmonics, but despite they still flow through the valves and the transformer windings, those harmonic currents are 180° out of phase, being canceled in the transformer's primary AC side. Thus, increasing the installation number of pulses is a great advantage to reduce dramatically the current harmonic

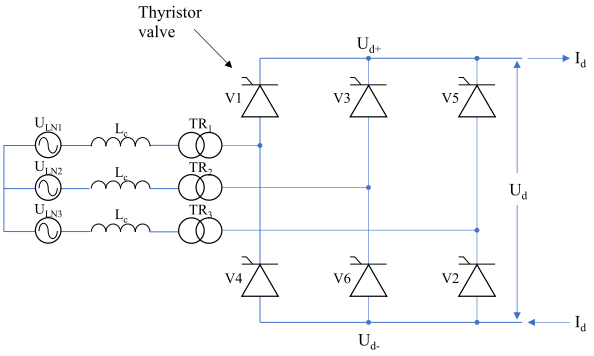

(a)

(b)

FIGURE 4. LCC six pulse bridge circuit (a) and valve connection inside the valve hall (b), authorized by Hitachi Energy.

content and, therefore, the filtering requirements compared to the 6-pulse solution.

The LCC technology requires a strong network connection to operate successfully, since the thyristors commutation are synchronized with the AC network. That avoids the voltage instability, but also does not permit LCC to be connected to an isolated load, like an offshore platform. The network strength is measured by the short-circuit ratio (SCR) which is the relation between the system short-circuit power by the converter station rated power [35].

Nowadays LCC installations are reaching DC voltage rates of ±1100kV and transmission power up to 12GW in projects like ChangJi-GuQuan [36], [37] and XinJiang-AnHui in China [38], [39].

The Fig. 5 displays how the HVDC application progressed along the years, in terms of rated voltage and power, and by its rapid growth in the last 25 years, picking some main projects for each period.

2) SELF-COMMUTATED VOLTAGE SOURCE CONVERTER

Self-commutated VSC (Figs. 6a and 6b) with pulse-width modulation (PWM) was introduced as a system solution in the 1990's. The increase in power and voltage ratings has enabled VSC to operate where, in the past, only LCC would be used. The VSC converters are self-commutated by an

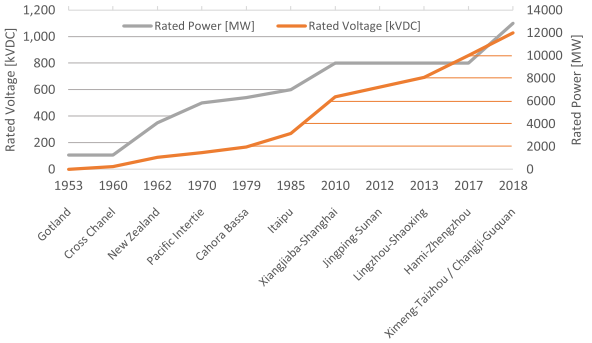

FIGURE 5. Development of HVDC technology along the years in terms of rated voltage and power, adopted from [40].

insulated-gate bipolar transistor (IGBT), connected to solid-dielectric extruded HVDC cables.

VSC permits a rapid control of the active and reactive power independently, controlled at each terminal, no mattering the DC transmission voltage level. This control flexibility allows VSC converters to be placed anywhere in the system, without restriction such as minimum network short circuit capacity. Self-commutation allows the converter to synthetize a balanced three-phase voltage which simulates the operation of a synchronous generator, using the control capability. The dynamic support of the AC voltage in each converter improves the voltage stability and permits a transferred power increase between sending and receiving ends, thereby extending the transfer capability of the DC link [41].

Projects like EuroAsia, EuroAfrica, mentioned in section I, and Western Link in UK, certify that VSC is suitable to transmit energy in DC voltages higher than ±500kV and rated powers over 2000MW. Due to the self-commutating characteristic, it has been widely used to connect offshore links to wind farms, supply oil and gas isolated platforms.

The Table 1 describes the HVDC implementation for each application according to the system topology. The Capacitor Commutated Converter (CCC) was not mentioned before. It is similar to the LCC topology, with a commutated capacitor placed between the converter transformer and the thyristor bridge. It gives a contribution for the valve voltage, allowing the operation at smaller firing angles, reducing the reactive power requirement, appearing to be less dependent on the AC network.

3) THE STANDARD FOR HVDC APPLICATION

The IEC/IEEE 60076-57-129 [42], titled Transformers for HVDC Application, has the first edition published in November 2017. It is a combination of the normative experiences brought by the formers IEEE C.57.129 and IEC 61378-2. The standard brings specific requirements related to losses, tests, sound level, components such as bushings and tap changer, some informative annexes related to overloading, transformers for VSC converters, design review, audible sound, and service load losses determination.

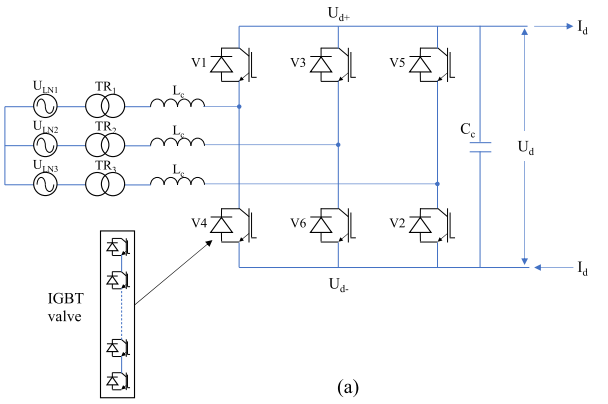

(a)

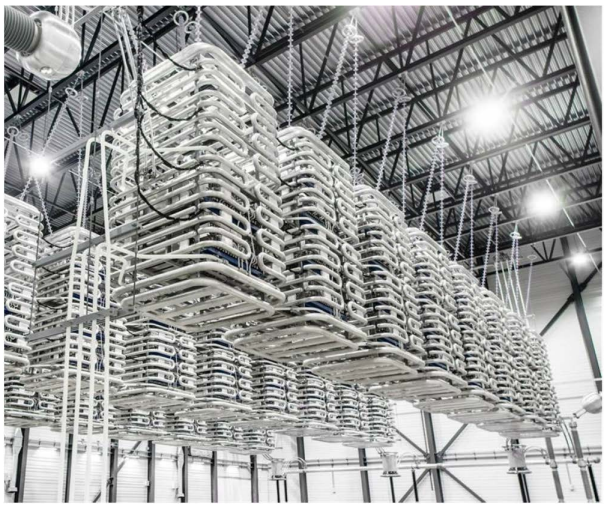

(b)

FIGURE 6. VSC six pulse bridge circuit (a) and valve connection inside the valve hall (b), authorized by Hitachi Energy.

TABLE 1. Application According to the System Topology.

	Long dist. land	Long dist. sea	Async. inter connect	Wind farm to network	Feed of isolated loads
LCC OH lines	X		X		
LCC sea cables		X	X		
CCC back-to-back			X		
CCC OH lines	X		X		
CCC sea cables		X	X		
VSC back-to-back			X	X	
VSC Land / sea cables	X	X	X	X	X

The scope of the standard [42] includes single or three-phase HVDC transformers of two, three or multiple windings and back-to-back applications. Industrial and traction transformers are excluded, being normalized by IEC 61378-1/ IEEE C57.18.10 and IEC 60310, respectively.

This article intends to point the main matters addressed by the standard and provide additional discussions found in an extensive literature research on each topic, with focus on the effects of the HVDC system operation over the converter transformer design. It has not the presumption to approach all subjects the technical standard presents, but it purposes to give the reader a comprehensive overview on the six main effects found in the standard, which are: transformer loading, load losses, sound level, thermal design, DC bias and electric field distribution, under an HVDC transformer design perspective. They are fully part of LCC operation, however VSC may also be susceptible to some, as in an asymmetric configuration or when the AC filters are not located between the converters and the transformers.

III. HVDC SYSTEM EFFECTS ON TRANSFORMERS

The converter transformer is the electrical link between the AC and DC transmission systems, responsible for part of the DC voltage regulation and permitting the reactive power control. The converter valves non-linearity operation causes some undesirable effects that demand a special design of the converter transformers [43].

Increasing technical margins not necessarily improve safety or life expectance, but it will surely reflect in the manufacturing costs. However, enough margins and a suitable design should be verified by a consistent design review [44]. Guidelines for such a revision can be found in [45] detailing checkpoints for specification requirements, system data, environmental conditions, transformer design, fabrication, inspection, test plan, transport, and installation.

A. HVDC TRANSFORMER LOADING

Since HVDC systems, specially LCC, transport high bulk energy and interconnect large power systems, the converter transformers normally operate under stressful load profiles. During normal operation, the valve switching provides a considerable harmonic content, that increases transformer losses and noise level. Also, overload cycles are usually specified in the technical documentation. Details of those effects and their undesirable consequences are given in the coming sections.

A fault in the DC line or in the DC yard may require the HVDC system to operate under a reduced voltage profile. That operational mode requires a larger thyristor firing angle $\alpha 2$, increasing losses and localized hots-spots, when compared to normal operation, angle $\alpha 1$, consuming more reactive power (Fig. 7).

1) IEC/IEEE 60076-57-129 HIGHLIGHTS

The converter transformer load current is composed by the fundamental frequency and harmonic orders. Their magnitudes depend on the converter station and include some residual DC components.

The HVDC system consumption of reactive power will penetrate the transformer windings, likewise the current harmonic content and any wave form distortion, which must be considered in the design. That information should be

analyzed in combination with the AC voltage and tap changer position [42].

Overloading the transformer in service is a result of the following events:

- Planned overloads
- Emergency overloads
- Failure of auxiliary equipment of the unit or the converter station

Any overload may result in significant reduction of the insulation life, increasing the risk of a failure. Planned overloads can be combined to a low ambient temperature profile or a limited duration capability.

The overload condition shall be informed with additional data as the ambient temperature, duration, overload factor [p.u.], preload [p.u.], number of coolers in service, permissible overtemperatures for oil, windings and hotspot, harmonic spectrum and tap changer position.

2) ADDITIONAL DISCUSSIONS

Transformers for LCC installations are normally specified with on-load tap changer. Despite the AC line voltage variation, which is limited by the standards between 5 and 10%, the tap changer is used to control the transformer valve side RMS voltage [46]. In combination with the thyristors firing angle, the transformer valve side voltage is used to control the amount and direction of the DC link power flow.

During normal operation, the converter α angle can be set for instance in 15° and the inverter γ angle in 17°. The transformer tap changer in the converter station transformer is set in a lower tap, resulting in a higher valve terminal voltage than the inverter station transformer. That defines a normal power flow from the converter to the inverter station and the power magnitude is a result of those parameters. During reverse operation, the pole voltage polarity is changed, in order to force the power flow to reverse [47], what stresses the transformer insulation by a combination of AC and DC stresses. That is tested by the polarity reversal test during the FAT (Factory Acceptance Tests). In reverse operation, normally the transmitted power is reduced due to the inverter's capacity limitations.

The HVDC transformer voltage regulating tap range is far wider than for power transformers. It is common to require more than 30% range above the nominal voltage, reflecting in a large regulating winding number of turns. This is used during reduced voltage profile, when the system DC voltage is required to be dropped around 70 to 80% of the nominal pole voltage. The thyristors' firing angle is set around 30°, resulting in a much higher current harmonic distortion, increasing the transformer losses and reactive power consumption [48]. During normal operation, the reactive power represents about 50% of the active system power [49], [50]. During reduced voltage operation this amount can reach more than 70%. A high reactive loading is relevant when the AC system requires to improve stability, transmission efficiency and HVDC conversion performance, controlling the steady-state and fast voltages transients [51]–[53]. The reactive loading can be seen by two perspectives: load compensation and voltage support [54].

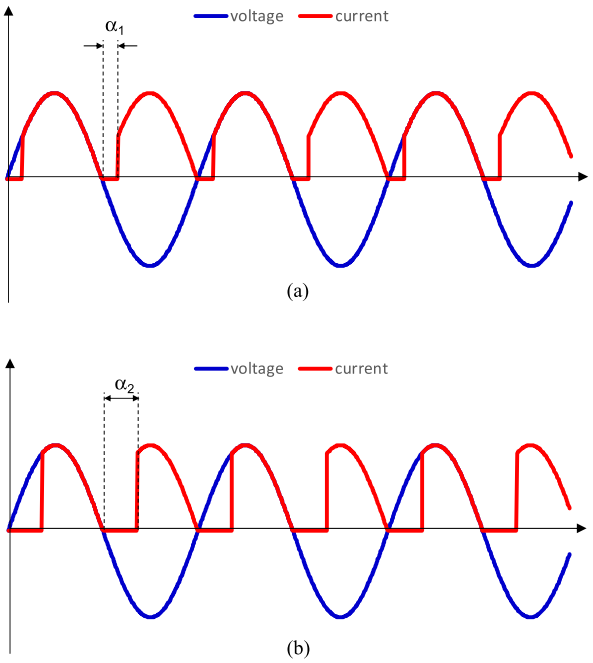

FIGURE 7. Single-phase full bridge wave form of an in-phase voltage and current considering a small (a) and large (b) thyristor firing angle.

During an overload, the firing angles are kept close to the ones practiced in normal operation or even lower, like 12°. That results in a less severe harmonic spectrum during overloads, but the current magnitudes can reach 133% for planned and 150% for emergency cycles. For a two-bipole installation those overloads represent the loss of one monopole or one bipole.

B. LOAD LOSSES CALCULATION

The converter transformer leakage flux contains some harmonic orders of the load current, increasing the additional load losses in the windings and in the internal metallic parts, such as core clamps, tank, flitch-plates and active part or tap-changer supports. This augmentation can be around 25 to 30% of the total load losses, resulting in local hotspots higher than in a conventional transformer operation, what may generate dissolved gases in oil [48], [55].

1) TECHICAL STANDARD HIGHLIGHTS

The winding rated current combines the fundamental with different harmonic components, which may change significantly from one converter installation to another.

The eddy losses are generated by the leakage flux impinging the winding conductors, creating a circulating current in the material. The same situation happens in other metallic parts, resulting the stray other-eddy losses [56]. The standard [42] gives a formulation for the total load losses

P_N described in (1):

$$P_N = I_{LN}^2 R + P_{WE1r} F_{WE} + P_{SE1r} F_{SE} \quad (1)$$

Being,
P_N: total load losses
P_{WE1r}: additional eddy losses
P_{SE1r}: additional stray other-eddy losses
The factors F_{WE} and F_{SE} are defined in (2) and (3) as:

$$F_{WE} = \sum_{h=1}^{49} k_h^2 h^2 \quad (2)$$

and

$$F_{SE} = \sum_{h=1}^{49} k_h^2 h^{0.8} \quad (3)$$

Being $k_h = \frac{I_h}{I_r}$ and $h = \frac{f_h}{f_1}$ which respectively represent the current ratio between the h^{th} and the rated currents, and the frequency ratio between the h^{th} and the fundamental frequencies.

It is possible to verify from (2) that the eddy losses dependency of the harmonic frequency by an exponent 2 and from (3), the stray losses by an exponent 0.8. That is an important information when measuring the load losses in different frequencies.

Considering all the current harmonic orders up to the 49^{th}, it is possible to calculate in (4) the rated current, which is the transformer load current for the nominal condition:

$$I_r = \sqrt{\sum_{h=1}^{49} I_h^2} \quad (4)$$

Different harmonic spectra can be informed to the manufacturer for several loading or overloading conditions. The spectra used for the heat-run test, performed in the highest current tap position, may not be the same than the one used for load losses evaluation. During heat-run test, an equivalent load current can be applied, as defined in (5):

$$I_{eq} = I_r \left(\frac{I_{LN}^2 R + P_{WE1r} F_{WE} + P_{SE1r} F_{SE}}{I_r^2 R + P_{WE1r} + P_{SE1r}} \right)^{0,5} \quad (5)$$

The no-load losses may be affected by voltage harmonics, but it is normally negligible when compared to the total losses. Nevertheless, DC-bias can significantly affect the no-load losses and it shall be considered in the design stage and the losses increase during heat-run test.

2) ADDITIONAL DISCUSSIONS

The standard method has been applied for factory testing along the years, but it may not represent completely the reality in service [57]. The load current in operation generates a nonlinear and non-sinusoidal leakage flux, which results in additional losses and located overheating [58].

The references [59]–[62] propose different methods for additional load losses calculation considering the winding inductance variation, material nonlinearity and hysteresis characteristics, frequency domain behavior and electromagnetic circuit coupling. According to the authors, those are deviation causes when calculated and measured losses are compared. For instance, the load current and the leakage flux should be represented for each harmonic order and simulated in a 2-D FEM (Finite Element Method) program to calculate winding eddy losses. The other-eddy losses should be calculated by a 3-D FEM program due to the active part and tank structure asymmetry [63]. Magnetic and nonmagnetic materials do not behave similarly for losses. That may also be a deviation cause, when a more detailed calculation is made, considering material hysteresis, nonlinearity behavior and frequency characteristics.

Some corrections and alternative formulations are proposed by [64]–[66] to adjust the technical standard factors. In fact, the losses calculation in HVDC transformers is being an issue and it has encouraged many authors to seek alternative methods to do it more accurate, considering effects such as skin and proximity, which are not covered by the traditional calculation [67].

C. THERMAL DESIGN

The transformer thermal behavior is defined by the losses' distribution inside the active part. In LCC installations, the harmonic filters are connected to the transformer AC terminal, so all converters nonlinearity components are driven directly to the valve winding.

1) TECHICAL STANDARD HIGHLIGHTS

Due to the frequency harmonic and DC current effects, the losses may not be evenly distributed along the winding height, like expected during the heat-run test [42]. So, in operation, hotspot locations and magnitudes may be significantly different [69]. The intense radial leakage flux generates high temperatures in the extreme winding discs or turns, represented by a multiplying constant called hotspot factor. The winding losses are calculated normally by a 2D-FEM software [70], considering the harmonic content, following the method described in section III.B.1.

The standard [71] proposes an indirect calculation method based on the mean winding-oil temperature gradient and the tank oil temperatures, using the hotspot factor to define the winding hotspot from calculated and measured temperatures. Higher hotspot factors are expected in converter transformers than in power transformers.

The hotspot temperature can be measured directly by placing fiber optic probes inside the transformer windings, especially at the main windings top discs or turns. The hotspots are located at a discrete and normally restricted region, so even defining a loss distribution calculation and an oil flow circulation, the designer cannot fully assure the fiber optic location will be placed exactly at the same region where the highest temperatures occur. It is not insured that the installation of one or two fiber optics sensors will detect relevant hotspot temperatures. Up to 10K difference were found on experiences with sensors located at windings top discs.

Additionally, probes can be placed in the core, between adjacent sheets and in other active part and tank locations where the hottest spots are expected. Those actions increase

the effectiveness of the measurements taken by the direct method.

Loads beyond nameplate shall be specified giving its duration, redundant cooling in operation (on/off), ambient temperature, DC and RMS currents and specific harmonic spectrum. The harmonic spectrum composition changes significantly depending on the different load profiles and may submit the transformer insulation to severe thermal stresses.

The standard [42] reports some side effects by loading a transformer beyond nameplate like, the insulation material gassing evolution, active part cellulose structure mechanical strength reduction, gaskets leaking, tap changer contacts premature wear, auxiliary equipment aging and excessive oil expansion, increasing tank internal pressure.

(a)

(b)

FIGURE 8. Converter transformer external thermal scan on tank during heat-run test, without (a) and with (b) thermal scan use of image authorized by Hitachi Energy.

Also, metallic structures may suffer localized saturation due to the high leakage flux magnitude, such as tank, tank shields, bushing turrets, core laminations, core clamps, tie-plates, yoke bolts, etc. Installing thermocouples to monitor metallic parts not directly in contact to the insulation, may be a recommended practice. The thermal behavior is verified externally by a thermal-scan during the heat-run test to check possible hotspot regions (Fig. 8).

2) ADDITIONAL DISCUSSIONS

All specific load harmonic content shall be informed, even those related to some specific load conditions, where the commutation angle is expected to be higher than the nominal. Overload and special applications might result in the transformer and its components life reduction, since hotspots can reach temperatures beyond the cellulose thermal limits, reducing its mechanical strength, causing a premature dielectric failure due to the insulation degradation along the operating life [72]–[74]. A complete failure report involving thermal, dielectric, and other failure causes is found in [75] which is an HVDC transformer failure survey, including back-to-back, with data collected along the years.

The DC voltage of a back-to-back installation is much lower than in a classic HVDC. Therefore, the valve windings are normally located next to the core. Furthermore, in a three-phase unit, both valve windings, delta and wye connected, may be manufactured in the same winding shell, like in a GSU (Generator Step Up) transformer axial split winding. But, due to the 30° phase displacement and the low reluctance, there is a considerable leakage flux radial component different than zero in region "A" of Fig. 9, between the two DC windings, directed to the core, resulting an overheating of the winding turns located in "B".

The investigation [76] verified that the delta winding insulation was more thermally stressed than the wye, since its strand dimension was 18% higher, suffering a greater overheating due to the higher losses. The reference also presents a calculation method fixing the leakage flux in the wye winding, Fig. 10(a), in 1.0pu, showing that the leakage flux in the delta reached $\pi/\sqrt{6} = 1.28$pu at fundamental 60Hz frequency, Fig. 10(b). The resulted RMS leakage flux in region "A" was 44.8% at the fundamental frequency, added to the other harmonics of higher frequency orders, showed in Fig. 10(c).

The thermally damaged winding insulation had the mechanical strength dramatically reduced, resulting in two 240MVA transformers dielectrically failed in service, followed by the spare unit gas generation, which was in operation just for 18 months, 15 of them under a reduced load of 180MVA. Simulations showed the hotspot reached 159°C on the damaged region, against the 120°C limit for thermally upgraded paper.

The failed units valve windings were redesigned with a smaller conductor height and removing the extra insulation used in region "A". The paper thickness was not a dielectric requirement, once the rated RMS voltage was only 23.3kV and there was enough distance between the two windings and from windings to core. In fact, it was reducing the copper-oil heat exchange capacity, contributing for the overheating in that region.

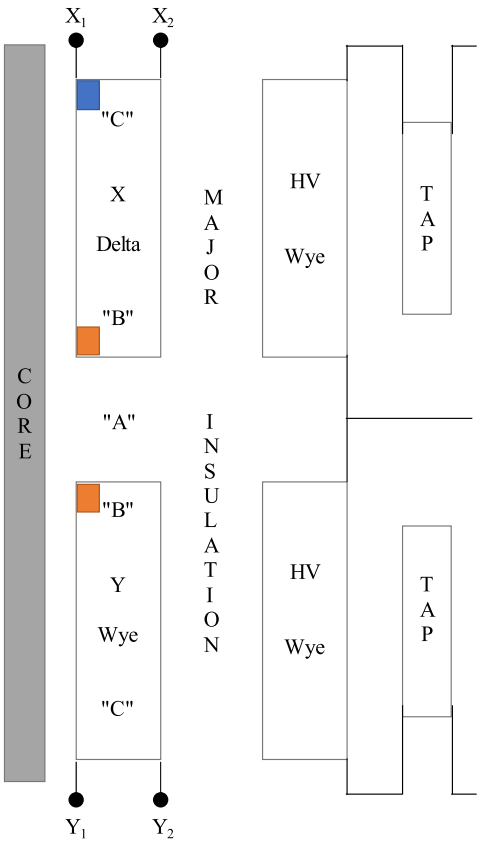

FIGURE 9. Back-to-back converter transformer winding arrangement per limb.

D. SOUND LEVEL

The converter transformer sound level under operation is a combination of many components:

- Core excitation at rated frequency
- Winding load current
- Harmonics in the load current and service voltage
- DC bias effect
- Cooling equipment

The complete sound level will be a combination of the different sound powers, obtained by a logarithm sum of all those components.

1) TECHICAL STANDARD HIGHLIGHTS

The sound level is expressed as the A-weighted of the total sound power, including all frequency bands or as the A-weighted sound level in 1/3 octave band. It is used to assure the total specified converter station sound level [42].

The core sound frequency spectrum consists mainly of the power of the even frequency harmonics. For 60Hz, it is represented by 120, 240, 360 and 480Hz [77].

The harmonic influence in the load audible sound occurs only in service and cannot be reproduced during the FAT due to unavailability of sufficient power supply in the manufactures facility to generate distorted wave shapes [42]. For a conventional transformer it consists mainly of twice the

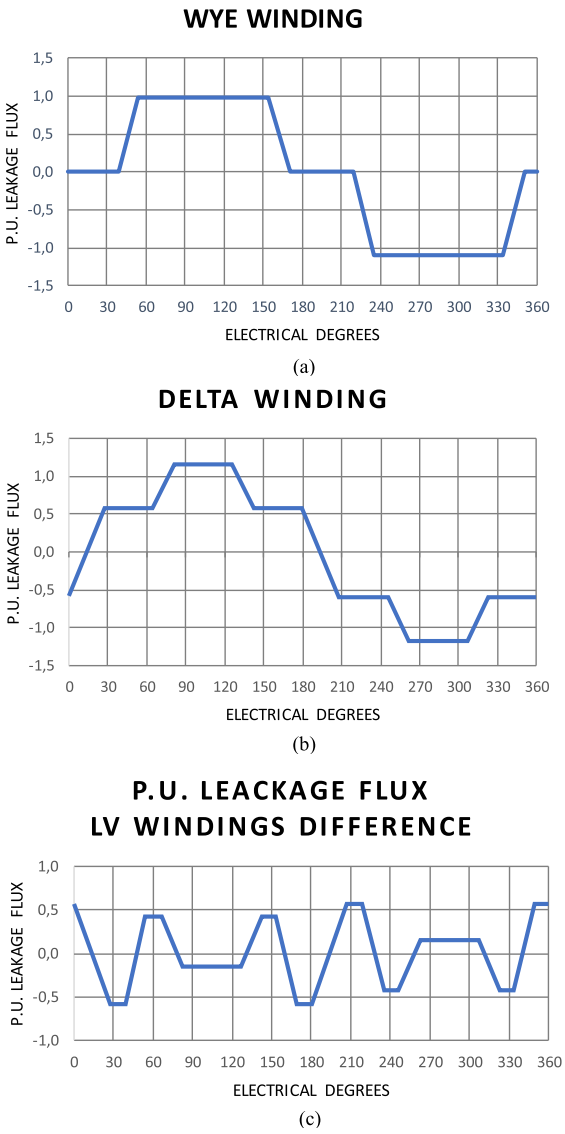

FIGURE 10. Valve windings wye (a) and delta (b) and difference (c) in leakage fluxes [p.u.].

power frequency, i.e., 120Hz for 60Hz [69]. For converter transformers it is associated to the converter harmonic spectrum in different frequencies.

The cooling system sound level shall be measured separately and added to the total sound calculation by a logarithmic sum. The frequency spectrum is defined by the motors' broadband, plus some discrete tones and harmonic content [77].

2) ADDITIONAL DISCUSSIONS

The core excitation refers to the magnetic circuit vibration, excited usually at rated voltage. Even though, the guarantee can be specified in other excitation condition, but always at rated frequency. It is defined by the core geometry (limb height, limb pitch and core diameter), the actual flux density and core steel type. The tank design can also influence if magnetic tank shunts and sand inside the stiffeners are used.

FIGURE 11. Oil to air cooler bank installed in an inverter station.

The windings vibration is defined by the load current and, in case of converter transformers, the current harmonic content [78]. It is defined by the windings' geometry (diameter, radial width, and total height), the conductor dimensions, the number of single strands or within a CTC (continuous transposed cable) cable in radial and axial directions, the number of spacers along the winding circumference and the winding block distance to tank.

Comparing a converter transformer to an equivalent power transformer, the sound level may vary from 2 to 30dB(A) higher. That because the converters non-linear operation combined with DC bias effect result in excessive windings and core vibration, far beyond the technical standards limits [78].

The cooling equipment is composed by fans, pumps, oil to air (Fig. 11) or oil to water coolers, depending on the transformer application, installation requirements or design choice.

The core, load and cooling system audible sound can be optimized by the designer, by choosing suitable materials or dimensions and distances, depending on the specified and environmental requirements. Some actions to minimize the total noise level are the use of high oriented grain or domain refined core steel, use low noise cooling fans, increase windings design space factor, increase windings to tank distances, consider sand inside the tank stiffeners, install external sound panels (Fig. 12a) or sound enclosures (Fig. 12b). These actions can drop down the sound level in more than 10 dB(A). The installation of sound panels or enclosures may increase the oil temperature rise, for the tank cooling capacity reduction.

E. DC BIAS EFFECT

A DC current flowing through the transformer winding is denominated DC bias current. It will create an offset of the rated core magnetization current showed in Fig. 13.

(a)

(b)

FIGURE 12. Sound panels (a) and enclosure (b) installation, use of image authorized by Mecart Transformer Screens and Enclosures [79].

Every electronic amplifier has some bias effect and HVDC valves are not an exception.

1) TECHICAL STANDARD HIGHLIGHTS

An unsymmetrical converter switching causes an uncompensated DC bias current, resulting in a half-cycle core saturation, showed in Fig. 13. DC bias affects the no-load losses, noise level and cooling design, however, the standard [42] mentions the losses increase can be neglected compared to the transformer total losses. DC bias effect cannot be verified by FAT, only in-service operation.

2) ADDITIONAL DISCUSSIONS

The returned DC current magnitude is typically assumed to be up to 10A in the neutral [42], [45]. It is created by a combination of the ground potential increase, called ground

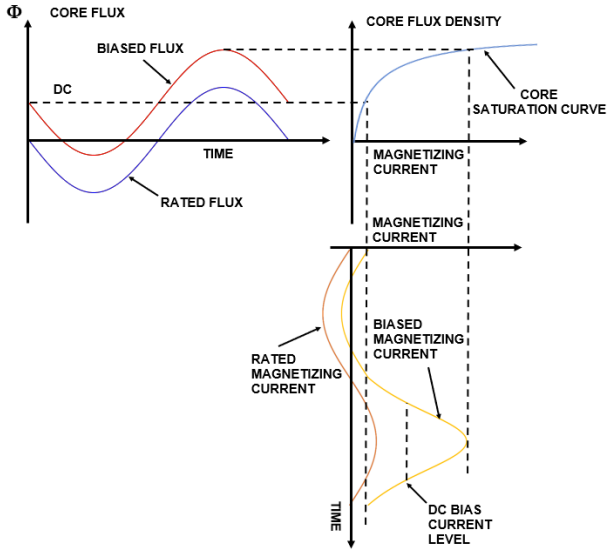

FIGURE 13. Flux density and magnetizing current behavior under DC bias effect, adopted from [80].

potential rise (GPR), an electromagnetic coupling effect and an unsymmetrical thyristor's firing operation. In this section, the first two causes will be detailed once the third one tends to be minimized by the operational control.

3) GPR – GROUND POTENTIAL RISE

The DC bias current sourced by the GPR results in a current return by the neutral terminal during monopolar, bipolar, or homopolar operation, under normal, emergency or fault conditions [81]. Any AC transformer or metallic utilities located in the surrounding area of the electrode or the converter stations, may be affected by the GPR. Returning currents can be measured in cooling pipes, cooling equipment, cabinets, and other accessories, causing premature corrosion.

The DC current magnitude is a function of the electrode configuration, ground geological composition [82] and installation distance from the HVDC electrode. It is simulated using different soil models, as horizontally layered, vertically layered or exponentially varying [83]. It is verified by two-electrode voltage difference (voltage source) and the analyzed AC system zero sequence resistance. With fewer substation transformers in operation and minimum AC system zero sequence resistance, which means, a maximum number of AC lines connected between the electrode stations, the maximum DC bias current will be sourced, and the highest magnitude will be reached. So, it will increase proportionally to the electrode surrounding AC system expansion.

The electrodes are usually constructed in two different configurations: Shallow Horizontal like ring (Fig. 14), n-pointed star, branched star and linear electrode arrangements, and Deep Vertical which consists in the interconnection of several deep conductors to reach the low resistance soil layers. The vertical electrode is used when the land dimensions do not allow a horizontal electrode installation. In [83], the maximum earth gradients given by the touch and step voltages are analyzed. It is also possible to verify the measured GPR for ring and 4-arm star electrode, for a 2000A ground return current and a soil layered in three layers of 50 ohm-m and 4m thickness in the top, 11 ohm-m and 18m in the middle, and a bottom layer of 260 ohm-m resistivity.

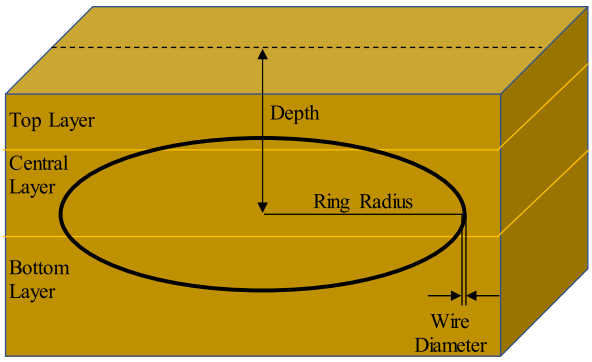

FIGURE 14. HVDC ground electrode and soil layers division.

The maximum voltages in the Tables 2 and 3 are achieved in distances below 800m for the ring pattern and below 1200m for the 4-arm star.

Currents up to 6.6Adc were measured along a 600-mile (966 kilometers) Pacific Gas Transmission and Electric Company pipeline located 35 miles (56.3 kilometers) far from Celilo electrode, which is part of Dalles-Los Angeles link in USA. The ground return transmitted current was 2000A [83].

The HVDC link connecting Talcher-II to Kolar station, through a 1370km 2000MW DC transmission line (±500kVdc, 2000A), had in 2003 an unexpected GPR registered right after a monopolar operation with ground return [84]. The cause was assigned to the geological composition and not directly to the electrode design.

GPR measurements in Hydro-Quebec's Radisson-Sandy Pond link showed magnitudes around 30Adc per phase in the Radisson substation 315kV converter transformers and 25Adc per phase in the 735kV autotransformers.

The reference [85] shows results of a DC current injection test in two single-phase autotransformers of 370MVA and 550MVA respectively, both 735kV at the HV. The current was injected in the tertiary winding in steps of 425, 850, 1700 and 2550A, resulting in 12.5, 25, 50 and 75A on the HV terminal. A voltage source varying between 0-55V, connected to a diode bridge, was capable for supplying a current up to 3000Adc. The measurements detect a significant increase in the core losses and magnetizing current peaks. It also verified the core structure flitch-plates losses and temperature rises.

Excessive current magnitudes shall be monitored and avoided for more than few minutes. The transformer design influences considerably the DC bias effects in the core. Three-limbed three-phase cores are less affected than a three-phase five-limbed or single-phase cores. That happens because a three-limb core design provides a higher zero sequence reluctance, dropping down the zero-sequence flux generated by a DC current. A smoother magnetization curve

TABLE 2. The Ring HVDC Electrode Design [83].

Electrode Characteristics Overall Radius: 300m; Conductor Radius: 0.3m; Depth: 3m Computation Results				
		Maximum		
GPR	Resistance	Earth Potential	Touch Voltage	Step Voltage
226.16 V	0.113 ohm	206.26 V	21.67 V	1.12 V

TABLE 3. The Star HVDC Electrode Design [83].

Electrode Characteristics Arm Length: 460m; Conductor Radius: 0.3m; Depth: 3m Computation Results				
		Maximum		
GPR	Resistance	Earth Potential	Touch Voltage	Step Voltage
224.02 V	0.112 ohm	212.2 V	58.26 V	3.514 V

withstands higher DC current than a stepped one. This behavior is related to the selected steel material. The reference [86] simulates and analyzes the DC current effect in a three-phase five-limbed core (three main and two return limbs) model in terms of magnetizing current, low harmonic orders increase and magnetic field intensity.

The GPR can be verified by the installation distance to the electrode, considering some parameters such as station GPR in volts, station GPR as a percentage of the DC GPR and magnetizing current peak as a percentage of the nominal value [87]. The parametric study presented in that reference considered a typical system under monopolar operation with ground return and all those parameters are analyzed in detail.

4) ELECTROMAGNETIC COUPLING EFFECT

The electrical system expansion may result in an AC and DC lines physical proximity and parallel length in the same right of way, causing an electromagnetic coupling [88]. That interaction results in an overvoltage on the DC system, higher than expected for a conventional DC link [89], creating a low-order harmonic interaction [90], a steady-state induction of fundamental frequency voltages [91] and a zero sequence fault currents induction [92].

The electromagnetic coupling of an AC line in normal operation induces a fundamental frequency AC circulating current along the DC coupled line. That current, driven into the thyristors of the converter or inverter station, is naturally switched to a DC current; which flowing through the HVDC transformer valve winding, causes an increment in the core saturation [93] and results in a core saturation instability [94].

The reference [95] presents a study of a typical AC line coupling effect over an LCC-MMC (multilevel modular converter) hybrid system (Fig. 15). The power was transmitted from Yunnan to Shanghai, in China, over a 1018km overhead line. The study set the parallel length between 20 and 200km and separation distance from 40 to 200m. The DC link transmits 3000MW at ±500kV and the AC system, 5000MW at 1000kV.

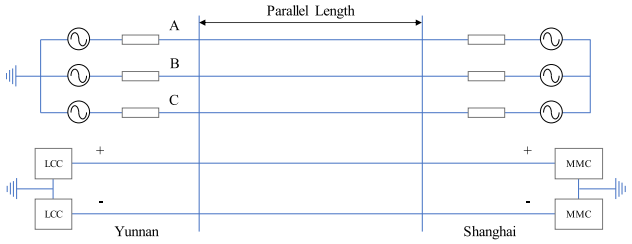

FIGURE 15. Parallel installation of HVDC and HVAC systems.

The line induced voltage was simulated varying the separation distance between 40 and 200 meters for a fixed line length of 100 kilometers, and the parallel length from 40 to 200 kilometers for a fixed separate distance of 100 meters (Fig. 16). The positive pole is closer to the AC line than the negative. That is why a higher voltage is induced in the positive line, more than 30kV for a separation distance of 40 meters, decreasing significantly for distances over 100 meters. The induced voltage does not show significant variation for distances over 140 meters.

The induced voltage is not proportional to the parallel length since the voltage is a function of the line inductance (self and mutual) and the coupling capacitance.

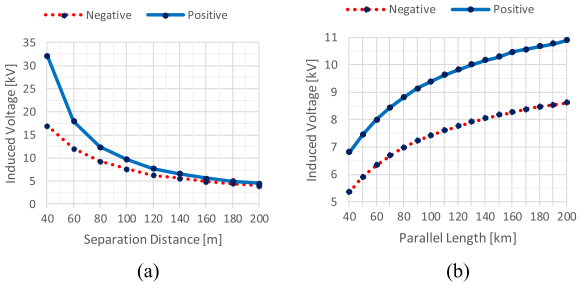

FIGURE 16. AC lines induced voltage on the DC lines under normal operation. (a) Induced voltage as a function of the separation distance. (b) Induced voltage as a function of the parallel length, adopted from [95].

The aim of the study is to verify the magnitude of the circulating current induced along the DC line connecting the rectifier LCC and the inverter MMC stations as a function of the separation distance and parallel length (Fig. 17). The shorter the separation distance, the greater the circulating current will be. For separation distances over 140m, the current magnitude does not change significantly.

The reference [96] does not recommend a circulating current higher than 30A. Considering that, the separation distance should be kept over 40 meters.

F. ELECTRIC FIELD DISTRIBUTION IN THE INSULATION SYSTEM

Besides the DC electric field distribution considerations, the dielectric design must consider transient effects such as:

- Polarity reversal for power flow inversion, causing an electric field disturbance for a short period, stressing the insulation system.

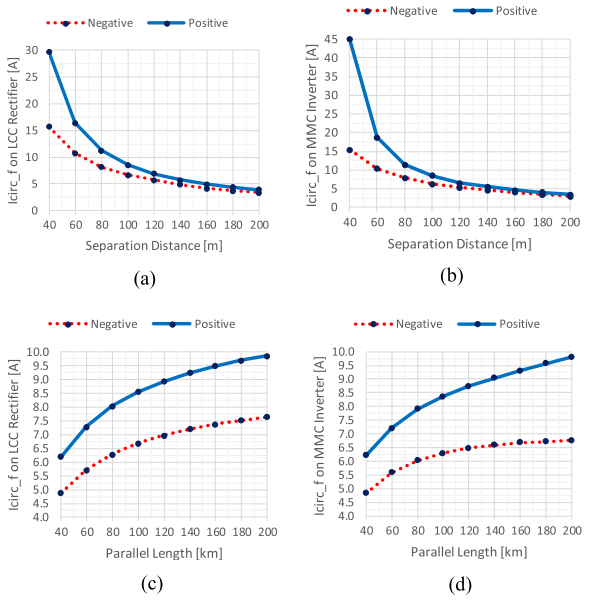

FIGURE 17. Icirc_f under normal operation. (a)-(b) Icirc_f as a function of the separation distance. (c)-(d) Icirc_f as a function of the parallel length, adopted from [95].

- Valve misfire in the converter station, creating oscillatory voltage surges in the valve windings.
- Converter station opened line switching, causing voltage surges with magnitudes up to 1.5pu of the rated voltage.
- Lightning impulses in the overhead lines reaching magnitudes around 2 or 3 times the system rated voltage, although being driven by the protective devices.

1) TECHICAL STANDARD HIGHLIGHTS

The transformer insulation system is mainly dielectrically stressed in service by the sources described above, extracted from [42] and [97], and FAT is the standard method to verify the insulation integrity and robustness [98]. The tests details listed below are found in [42] and [99]:

- Lightning Impulse
- Induced and Applied Switching Impulse
- Applied AC Voltage
- Applied DC Voltage
- Induced Voltage with PD Measurements
- Polarity Reversal

The applied tests are performed during a long duration period, combined with partial discharge (PD) measurement, intending to simulate the DC and AC stresses in the valve side during converting operation. In a similar way, Polarity Reversal simulates the LCC system operation reversal by changing the DC voltage polarity, combining the direct and alternating stresses.

2) ADDITIONAL DISCUSSIONS

The valve windings are exposed to the converter operational DC voltage component [100]. By using a 2D-FEM program and analytical equations, the Laplacian AC field is precisely obtained, once there are no free chargers, resulting in a quasi-stationary situation, from a capacitive distribution, where the curl of the electric field is null [101] and [102]. Furthermore, that behavior is similar to the conductivity, stressing the solid insulation more than the oil [103], differently than the AC fields.

Temperature and moisture cause little variation in the main material parameters such as permittivity and conductivity in AC field analysis. It is considered negligible for practical purposes, once the insulation materials are properly stored, well dried and oil impregnated. Furthermore, the relative insulation permittivity varies between 2.0 and 7.0.

On the other hand, the insulation performance for DC fields is considerably affected by temperature and moisture, which shall be well controlled during manufacturing process, once the permittivity and conductivity are exponentially influenced by those variables [104]–[106].

The materials breakdown characteristics under different voltage stress cases are analyzed by the following electric field equations. Considering the applied voltage $V(t)$:

$$\nabla \times \vec{H} = \vec{J} + \frac{\partial \vec{D}}{\partial t} \tag{6}$$

Applying the divergence in both sides of (6) and introducing constitutive relations to the current and electric density vectors, the equation can be re-written as in (7):

$$\nabla \cdot (-\sigma \nabla V) + \nabla \cdot \frac{\partial}{\partial t} (-\varepsilon \nabla V) = 0 \tag{7}$$

Replacing the electric field by the gradient of the potential $V(t)$, (7) turns into a double Laplacian equation, once the vector identity makes a gradient of a divergency swap to a Laplacian operator. The derivative in time and a constant portion established by the conductivity are defined in (8).

$$\sigma \nabla^2 V + \varepsilon \frac{\partial}{\partial t} \nabla^2 V = 0 \tag{8}$$

The DC voltage can be defined as a long-time energization in steady state [107]–[109] and a simplification is done taken $\sigma \nabla^2 V = 0$, whereas derivatives in time are null.

For a sinusoidal excitation $V(t) = V_o \sin(\omega t)$, the angular frequency times the permittivity becomes considerably large when compared to the conductivity. The time dependent field equation portion is shown in (9), while the voltage is not time dependent.

$$\varepsilon \frac{\partial}{\partial t} \nabla^2 V_{(x,y,z)} \sin(\omega t) = 0 \tag{9}$$

and

$$\varepsilon \omega \cdot cos(\omega t) \nabla^2 V_{(xyz)} = 0 \tag{10}$$

From (10), after a derivative operation, it is noted that the permittivity rules the potential distribution in an AC field configuration, while the insulation materials excitation voltage defines the DC field distribution.

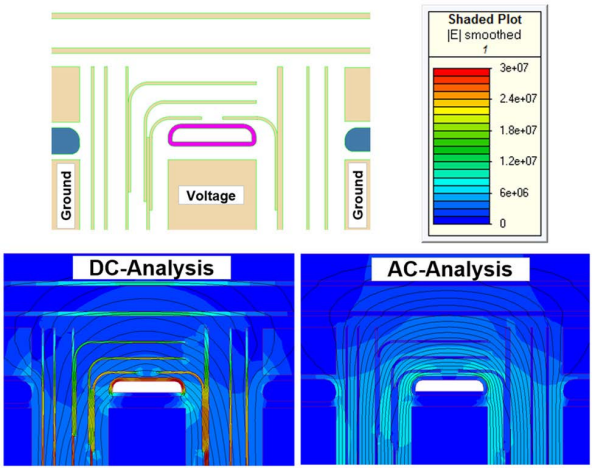

FIGURE 18. DC and AC field distribution inside an insulation structure.

3) DC × AC FIELD DISTRIBUTION PLOT

In this section, the authors used the same insulation structure, Fig. 18, to apply 680kVdc and 520kVac test voltages, using a 2D-FEM software. The electric field strength is represented by the shaded color and the equipotential voltage lines by the contours. The electric field distribution is influenced by the space charge established on the insulation, which defines the insulation dielectric strength in the windings, from the active part to the grounded parts, in the connections and between windings [110]. The simulation confirms the behavior mentioned previously.

4) VOLTAGE HARMONICS INFLUENCE

The technical standard [42] states that the voltage harmonics can affect the no-load losses, but it is negligible compared to total losses magnitude. Looking by an electrical field perspective, the reference [111] warns of a combination of the voltage harmonics with partial discharges and other dielectrics stresses superimposed, which not only distort the valve winding voltage waveshape, but also contribute with the insulation degradation [59], [112]–[117].

In [111], a voltage harmonic spectrum is analyzed considering $3k, 6k, 6k \pm 1, 12k$ and $12k \pm 1$ harmonic orders, where k is an integer from $1 \ldots n$, for the Huainan Converter Station in China which is rated in ±800kVdc and 6400MW. The THD (Total Harmonic Distortion) in percentage is given in Table 4, for the simulated and measured results, considering Y/Y and Y/D transformer winding connections.

A 3-D model was developed to analyze the electrical field inhomogeneity into the minor insulation, by a FEM simulation, especially along the valve winding electrostatic shield ring. It is enhanced by the voltage harmonics and insulation regions closer to the winding presenting higher voltage derivatives (dV/dt). Such derivatives can enlarge the partial discharges magnitude and accelerate the insulation degradation. Furthermore, defects found into the insulating material presented higher PD levels under voltage harmonics influence.

TABLE 4. Simulated and Measured THD [%] Results.

Harmonic Distortion				
	Simulated		Measured	
Connection	Y/Y	Y/D	Y/Y	Y/D
THD [%]	45.57	44.36	36.79	36.37

The voltage harmonics can also be a source for commutation failure and outages during the bipole reversal of polarity [118], [119]. The Cigré report [120] informs that 14 out of 22 failures in HVDC transformers occur in the valve winding. State Grid and China South Power Grid have registered thirty failures in operation from 2016 until now, due to severe operational conditions [111]. Thus, voltage harmonics are an issue that may compromise the converter transformer insulation dielectric withstand capability along the operation, requiring a consistent design of the solid insulation between windings and toward the core yokes, combined with satisfactory quality control to avoid undesired material defects.

IV. CONCLUSION

This paper provides the reader a comprehensive overview on how the HVDC system operation affects the converter transformer design, covering the technical standard IEC/IEEE 60076-57-129 highlights and including additional discussions found in an extensive search on the literature. The authors believe this article shades light and amplifies the view on the consequences of each effect and to help the readers know how to mitigate then through practical design solutions. The authors also included a comparison of the electrical field behavior under DC and AC stresses, via a finite element simulation, that shows the most stressed parts on the insulation where a reinforcement should be verified.

Those main effects must be considered during technical specification conception and checked by a design review audit. The way the design solutions deal with those effects can be determinant to validate the most optimized proposal and to assure the transformer will perform satisfactorily. The power systems expansion and interconnection worldwide are increasing the distances, power, and transported energy, reaching continental scales. Thus, the electrical, thermal, magnetic, and mechanical stresses tend to increase, and the transformer design to become more complex, requiring a great technical knowledge to specify and verify those requirements.

REFERENCES

[1] M. Bahrman, "Overview of HVDC transmission," in *Proc. IEEE PES Power Syst. Conf. Expo.*, Nov. 2006, pp. 18–26.

[2] Federal Ministry for Economic Affairs and Energy. (May 2017). *Concluding Paper: Electricity 2030—Long-Term Trends—Tasks for the Coming Years*. [Online]. Available: https://www.bmwi.de/Navigation/DE/Home/home.html

[3] *Global Energy & CO_2 Status Report-2017*, Int. Energy Agency, Paris, France, Mar. 2018.

[4] A. Kalair, N. Abas, and N. Khan, "Comparative Study of HVAC and HVDC transmission Systems," *Renew. Sustain. Energy Rev.*, no. 59, pp. 1653–1675, Feb. 2016.
[5] B. Van Eeckhout, D. Van Hertem, M. Reza, K. Srivastava, and R. Belmans, "Economic comparison of VSC HVDC and HVAC as transmission system for a 300 MW offshore wind farm," *Eur. Trans. Electr. Power*, vol. 20, pp. 661–671, Jul. 2010.
[6] G. F. Reed, H. A. A. Hassan, M. J. Korytowski, P. T. Lewis, and B. M. Grainger, "Comparison of HVAC and HVDC solutions for offshore wind farms with a procedure for system economic evaluation," in *Proc. IEEE Energytech*, May 2013, pp. 1–7.
[7] L. Weimers, "Bulk power transmission at extra high voltages, a comparison between transmission lines for HVDC at voltages above 600 kV DC and 800 kV AC," *Indian J. Power River Valley Develop.*, vol. 61, no. 7, p. 107, 2011.
[8] D. S. Carvalho, J. M. Bressane, M. Cury, T. C. Rizzotto, D. J. T. Souza, R. T. A. Mello, and R. R. Cabral, "An 800 kV HVDC bipole to reinforce a regional interconnection and integrate a large amount of variable renewable generation," B4-101 DC Syst. Power Electron., CIGRE, Paris, France, Tech. Rep. B4-101, 2018.
[9] M. Edmonds and T. Miller, "The next 50 years, what's next for the grid?" *IEEE Power Energy Mag.*, vol. 12, no. 2, pp. 92–96, 2014.
[10] A. Elahidoost and E. Tedeschi, "Expansion of offshore HVDC grids: An overview of contributions, status, challenges and perspectives," in *Proc. IEEE 58th Int. Sci. Conf. Power Electr. Eng. Riga Tech. Univ. (RTUCON)*, Oct. 2017, pp. 1–7.
[11] B. R. Andersen, "HVDC transmission-opportunities and challenges," in *Proc. 8th IEE Int. Conf. AC-DC Power Transmiss.*, Mar. 2006, pp. 24–29.
[12] *Assessment of the Potential for High-Voltage Direct Current Transmission to Mitigate Impacts of Non-Dispatchable Generation Technologies—Final Report*, Energy Inf. Admin., Washington, DC, USA, Mar. 2018.
[13] S. L. Teichler and I. Levitine, "HVDC transmission: A path to the future?" *Electr. J.*, vol. 23, no. 4, pp. 27–41, May 2010.
[14] M. P. Bahrman, "HVDC transmission overview," in *Proc. IEEE/PES Transmiss. Distrib. Conf. Expo.*, Apr. 2008, pp. 1–7.
[15] R. Rudervall, J. P. Charpentier, and R. Sharma, "High voltage direct current (HVDC) transmission systems technology review paper," in *Proc. Energy Week*, Mar. 2000, pp. 1–19.
[16] R. Majumder, C. Bartzsch, P. Kohnstam, E. Fullerton, A. Finn, and W. Galli, "Magic Bus: high-voltage DC on the new power transmission highway," *IEEE Power Energy Mag.*, vol. 10, no. 6, pp. 39–49, Nov. 2012.
[17] D. Van Hertem, M. Ghandhari, and M. Delimar, "Technical limitations towards a SuperGrid—A European prospective," in *Proc. IEEE Int. Energy Conf.*, Dec. 2010, pp. 302–309.
[18] K. Meah and S. Ula, "Comparative evaluation of HVDC and HVAC transmission systems," in *Proc. IEEE Power Eng. Soc. Gen. Meeting*, Jun. 2007, pp. 1–5.
[19] J. Setreus and L. Bertling, "Introduction to HVDC technology for reliable electrical power systems," in *Proc. 10th Int. Conf. Probablistic Methods Appl. Power Syst.*, May 2008, pp. 1–8.
[20] Siemens AG. *HVDC Classic—Powerful and Economical*. Accessed: Jan. 8, 2022. [Online]. Available: https://assets.siemens-energy.com/siemens/assets/api/uuid:8572c795-95c7-49e8-8367-dc578b4e59a5/2021-09-27-hvdc-classic.pdf
[21] *List of HVDC Projects*. Accessed: Jan. 8, 2022. [Online]. Available: https://en.wikipedia.org/wiki/List_of_HVDC_projects
[22] *Reference List Hitachi Energy*. Accessed: Jan. 8, 2022. [Online]. Available: https://www.hitachienergy.com/offering/product-and-system/hvdc
[23] *Projects List SGCC*. Accessed: Jan. 8, 2022. [Online]. Available: http://www.sgcc.com.cn/ywlm/projects/index.shtml
[24] *Reference List LCC Siemens AG*. Accessed: Jan. 8, 2022. [Online]. Available: https://www.siemens-energy.com/global/en/offerings/power-transmission/portfolio/high-voltage-direct-current-transmission-solutions/hvdc-classic.html
[25] *Reference List VSC Siemens AG*. Accessed: Jan. 8, 2022. [Online]. Available: https://www.siemens-energy.com/global/en/offerings/power-transmission/portfolio/high-voltage-direct-current-transmission-solutions/hvdc-plus.html
[26] *Reference List GE*. Accessed: Jan. 8, 2022. [Online]. Available: https://www.gegridsolutions.com/systems_services/catalog/hvdc/
[27] M. G. Bennett and N. S. Dhaliwal, "A survey of the reliability of HVDC systems throughout the world during 2015–2016," B4-137 DC Syst. Power Electron., CIGRE, Paris, France, Tech. Rep. B4-137, 2018.
[28] *Protocol for Reporting the Operational Performance of HVDC Transmission Systems*, CIGRE, Paris, France, Jul. 2014.
[29] M. G. Bennett, N. S. Dhaliwal, and A. Leirbukt, "A survey of the reliability of HVDC systems throughout the world during 2011–2012," in *Proc. 44th CIGRE Session Paris*, Paris, France, 2014, pp. 1–9.
[30] M. G. Bennett and N. S. Dhaliwal, "A survey of the reliability of HVDC systems throughout the world during 2013–2014," CIGRE Session, Paris, France, CIGRE Report B4-131, 2016.
[31] *Analysis of HVDC Thyristor Converter Transformer Performance*, Joint Task Force B4.04/A2-1, CIGRE, Paris, France, Feb. 2004.
[32] *HVDC Converter Transformer Failure Survey Results from 2003 to 2012*, CIGRE, Paris, France, Apr. 2015.
[33] N. S. Dhaliwal, "Transformer failure survey report covering 2015 and 2016," CIGRE Session, Paris, France, CIGRE Report B4 AG04, Sep. 2017.
[34] X. Zhang, Z. Wu, M. Hu, X. Li, and G. Lv, "Coordinated control strategies of VSC-HVDC-based wind power systems for low voltage ride through," *Energies*, vol. 8, no. 7, pp. 7224–7242, Jul. 2015.
[35] *Off-Shore Transmission Technology*, Eur. Netw. Transmiss. Syst. Operators Electr., Brussels, Belgium, Nov. 2011.
[36] D. Wu, A. Kumar, M. G. Berglund, E. Organero, B.-O. Stenestam, and D. G. Gustavsson, "Challenges in bringing UHVDC from ±800 kV to higher voltages," CIGRE Session, Paris, France, CIGRE Report B4-116, 2018.
[37] R. Wimmer, R. Fritsche, T. Hammer, W. Kutzleb, K. Loppach, L. Zheong, and Z. Jin, "Introduction of a new level of HVDC to UHVAC linked systems with respect to main component transformer technology and design," CIGRE Report B4-126, 2018.
[38] L. Zehong, G. Liying, Y. Jun, Z. Jin, and L. Licheng, "Research work of ±1100 kV UHVDC technology," CIGRE Report B4-105, 2014.
[39] L. Zehong, G. Liying, W. Zuli, Y. Jun, Z. Jin, and L. Licheng, "R&D progress of ±1100 kV UHVDC technology," CIGRE Session, Paris, France, CIGRE Report B4-201, 2012.
[40] M. Berglund, M. Pettersson, T. Freyhult, and R. Montano. *White Paper: Developments in UHVDC and UHVAC Transmission*. [Online]. Available: https://search.abb.com/library/Download.aspx?DocumentID=1LAB%20000603&LanguageCode=en&DocumentPartId=&Action=Launch
[41] M. B. Bahrman and B. K. Johnson, "The ABCs of HVDC transmission technology," *IEEE Power Energy Mag.*, vol. 5, no. 2, pp. 32–44, Mar./Apr. 2007.
[42] *Power Transformers—Transformers for HVDC Applications*, Standard IEC/IEEE 60076-57-129, Nov. 2017.
[43] M. V. Czernorucki, M. B. C. Salles, A. S. Melo, E. C. M. da Costa, and L. Piegari, "Effects of the HVDC system on converter transformers," in *Proc. 8th Int. Conf. Renew. Energy Res. Appl. (ICRERA)*, Nov. 2019, pp. 623–630.
[44] "HVDC converter transformers design review, test procedures, ageing evaluation and reliability in service," CIGRÉ Joint Work. Group, CIGRE, Paris, France, Tech. Rep., JWG A2/B4.28, Feb. 2010.
[45] "HVDC converter transformers guidelines for conducting design reviews for HVDC converter transformers," CIGRÉ Joint Work. Group, CIGRE, Paris, France, Tech. Rep., JWG A2/B4.28, Feb. 2010.
[46] M. Sanjo, M. Jeffin, J. Sajan, and A. Deepak, "Power electronic on-load tap changer for HVDC converter transformer," *Int. J. Innov. Res. Elect., Electron., Instrum. Control Eng.*, vol. 7, no. 4, pp. 50–58, Apr. 2019.
[47] H. Dai, Y. Wang, X. Li, Z. Ming, and H. Deng, "Characteristic analysis of reactive power compensation device at HVDC converter station," in *Proc. Asia–Pacific Power Energy Eng. Conf.*, Mar. 2012, pp. 1–5.
[48] B. S. Ram, J. A. C. Forrest, and G. W. Swift, "Effects of harmonics on converter transformer load losses," *IEEE Trans. Power Del.*, vol. PWRD-3, no. 3, pp. 1059–1066, Jul. 1988.
[49] H. Yakupoglu, H. Gozde, and M. C. Taplamacioglu, "Technical and economic comparison of HVDC converter technologies," *Int. J. Tech. Phys. Problems Eng.*, vol. 10, no. 37, pp. 25–30, Dec. 2018.
[50] M. Bahrman, "HVDC technology line commutated converters," in *Proc. IEEE/PES Transmiss. Distrib. Conf. Expo. (T&D)*, Apr. 2014, pp. 1–31.
[51] A. Hammad and B. Roesle, "New roles for static VAR compensators in transmission systems," *Brown Boveri Tech.*, vol. 73, pp. 314–320, Jun. 1986.
[52] N. Grudinin and I. Roytelman, "Heading off emergencies in large electric grids," *IEEE Spectr.*, vol. 34, no. 4, pp. 42–47, Apr. 1997.
[53] C. W. Taylor, "Improving grid behaviour," *IEEE Spectr.*, vol. 36, no. 6, pp. 40–45, Jun. 1999.

[54] L. Yong, L. Longfu, C. Rehtanz, S. Ruberg, and L. Fusheng, "Realization of reactive power compensation near the LCC-HVDC converter bridges by means of an inductive filtering method," *IEEE Trans. Power Electron.*, vol. 27, no. 9, pp. 3908–3923, Sep. 2012.

[55] *Load Loss in HVDC Converter Transformers*, Electra, CIGRE, Paris, France, 1997, pp. 53–57.

[56] M. J. Heathcote, *The J&P Transformer Book*, 12th ed. Oxford, U.K.: Reed Educ. Prof. Publishing, 1998.

[57] Y. Li, L. Luo, C. Rehtanz, K. Nakamura, J. Xu, and F. Liu, "Study on characteristic parameters of a new converter transformer for HVDC systems," *IEEE Trans. Power Del.*, vol. 24, no. 4, pp. 2125–2131, Oct. 2009.

[58] A. A. Elmoudi, "Evaluation of power system harmonic effects on transformers: Hot spot calculation and loss of life estimation," Ph.D. dissertation, Dept. Elect. Commun. Eng., Helsinki Univ. Technol., Espoo, Finland, 2006.

[59] Y. Liu, D. Zhang, Z. Li, Q. Huang, B. Li, M. Li, and J. Liu, "Calculation method of winding eddy-current losses for high-voltage direct current converter transformers," *IET Electr. Power Appl.*, vol. 10, no. 6, pp. 488–497, Jul. 2016.

[60] J. A. C. Forrest, "Harmonic load losses in HVDC converter transformers," *IEEE Trans. Power Del.*, vol. 6, no. 1, pp. 153–157, Jan. 1991.

[61] Y. Wang, W. Zhang, J. Wang, D. Xia, P. Zhang, and J. Li, "Stray loss calculation of HVDC converter transformer," *IEEE Trans. Appl. Supercond.*, vol. 22, no. 3, pp. 550–554, Jun. 2012, Art. no. 5500604.

[62] Y. Liu, D. Zhang, Z. Li, Q. Huang, M. Li, B. Li, and J. Liu, "Evaluation of the calculation method for stray losses in structural parts of HVDC converter transformers," in *Proc. 5th Int. Conf. Electr. Utility Deregulation Restructuring Power Technol. (DRPT)*, Nov. 2015, pp. 1780–1785.

[63] W. F. Zhang, J. M. Wang, W. Q. Ge, P. Zhang, C. Y. Jing, and Y. H. Wang, "Calculation of additional loss for HVDC converter transformer," *High Voltage App.*, vol. 47, no. 7, pp. 18–23, Jul. 2011.

[64] A. Elmoudi, M. Lehtonen, and H. Nordman, "Corrected winding eddy-current harmonic loss factor for transformers subject to nonsinusoidal load currents," *IEEE Russia Power Tech*, Jun. 2005, pp. 1–6.

[65] S. N. Makarov and A. E. Emanuel, "Corrected harmonic loss factor for transformers supplying nonsinusoidal load currents," in *Proc. 9th Int. Conf. Harmon. Quality Power*, vol. 1, Oct. 2000, pp. 87–90.

[66] P. L. Dowell, "Effects of eddy currents in transformer windings," *Proc. Inst. Electr. Eng.*, vol. 113, no. 8, pp. 1387–1394, Aug. 1966.

[67] J. Faiz, M. Ghazizadeh, and H. Oraee, "Derating of transformers under non-linear load current and non-sinusoidal voltage—An overview," *IET Electr. Power Appl.*, vol. 9, no. 7, pp. 486–495, Aug. 2015.

[68] J. Liu and L. Luo, "Vibration and noise characteristics of the inductive filtering converter transformer," *Electron. Lett.*, vol. 53, no. 10, pp. 678–679, May 2017.

[69] L. W. Pierce, "Transformer design and application considerations for nonsinusoidal load currents," *IEEE Trans. Ind. Appl.*, vol. 32, no. 3, pp. 633–645, May/Jun. 1996.

[70] C. Jing, J. Wang, Z. Chen, and Z. Wu, "Analysis of transient leakage field and harmonic losses in windings of converter transformers," *Transformer*, vol. 44, no. 4, pp. 1–4, 2007.

[71] *Loading Guide for Mineral-Oil-Immersed Power Transformers*, Standard IEC 60076-7, Jan. 2018.

[72] G. Bhuvaneswari and B. C. Mahanta, "Analysis of converter transformer failure in HVDC systems and possible solutions," *IEEE Trans. Power Del.*, vol. 24, no. 2, pp. 814–821, Apr. 2009.

[73] D. H. Grant and W. McDermid, "Assessment of thermal aging of HVDC converter transformer insulation," in *Proc. Conf. Rec. IEEE Int. Symp. Electr. Insul.*, Sep. 2004, pp. 230–232.

[74] *Study of Converter Transients Imposed on the HVDC Converter Transformers*, CIGRE, Paris, France, Feb. 2015.

[75] *HVDC LCC Converter Transformers Converter Transformer Failure Survey Results from 2003 to 2012*, CIGRE, Paris, France, Apr. 2015.

[76] J. A. C. Forrest and B. Allard, "Thermal problems caused by harmonic frequency leakage fluxes in three-phase, three-winding converter transformers," *IEEE Trans. Power Del.*, vol. 19, no. 1, pp. 208–213, Jan. 2004.

[77] *Standard Test Code for Liquid-Immersed Distribution, Power, and Regulating Transformers*, Standard IEEE C57.12.90, Dec. 2015.

[78] P. Shao, L. Luo, Y. Li, and C. Rehtanz, "Electromagnetic vibration analysis of the winding of a new HVDC converter transformer," *IEEE Trans. Power Del.*, vol. 27, no. 1, pp. 123–130, Jan. 2012.

[79] *Mecart Acoustic Solutions*. Accessed: Jan. 8, 2022. [Online]. Available: https://mecart.com

[80] P. Hurlet and F. Berthereau, "Impact of geomagnetic induced currents on power transformer design," in *Proc. IEEE Conf. MATPOST*, vol. 7, 2007.

[81] *HVDC Ground Electrode Design*, document EPRI EL-2020, Aug. 1981.

[82] P. F. Freire and S. Y. Pereira, "HVDC ground electrodes and tectonic settings," CIGRE, Paris, France, Tech. Rep., B4-102, 2018.

[83] J. Liu, F. P. Dawalibi, J. Ma, and R. D. Southey, "HVDC advanced analysis methods for grounding design and DC interference mitigation techniques," in *Proc. 3rd Int. Symp. Electromagn. Compat.*, May 2002, pp. 202–206.

[84] R. N. Nayak, R. P. Sasmal, S. Sen, B. Pelly, and P. Riedel, "Experience with blocking devices during monopolar operation of ±500 kV, 2000 MW Talcher–Kolar HVDC system in India," *Cigré Session*, vol. 41, p. 204, Sep. 2006.

[85] P. Picher, L. Bolduc, A. Dutil, and V. Q. Pham, "Study of the acceptable DC current limit in core-form power transformers," *IEEE Trans. Power Del.*, vol. 12, no. 1, pp. 257–265, Jan. 1997.

[86] X. Li, X. Wen, P. N. Markham, and Y. Liu, "Analysis of nonlinear characteristics for a three-phase, five-limb transformer under DC bias," *IEEE Trans. Power Del.*, vol. 25, no. 4, pp. 2504–2510, Oct. 2010.

[87] A. P. S. Meliopoulos and G. Christoforidis, "Effects of DC ground electrode on converter transformers," *IEEE Trans. Power Del.*, vol. 4, no. 2, pp. 995–1002, Apr. 1989.

[88] T. Jian, Z. Rong, M. Hongbin, H. Jinliang, Z. Jie, L. Xiaolin, and W. Qi, "Analysis of electromagnetic interference on DC line from parallel AC line in close proximity," *IEEE Trans. Power Del.*, vol. 22, no. 4, pp. 2401–2408, Oct. 2007.

[89] R. Verdolin, A. M. Gole, E. Kuffel, N. Diseko, and B. Bisewski, "Induced overvoltages on an AC-DC hybrid transmission system," *IEEE Trans. Power Del.*, vol. 10, no. 3, pp. 1514–1524, Jul. 1995.

[90] E. V. Larsen, D. H. Baker, and J. C. McIver, "Low-order harmonic interactions on AC/DC systems," *IEEE Trans. Power Del.*, vol. 4, no. 1, pp. 493–501, Jan. 1989.

[91] E. V. Larsen, R. A. Walling, and C. J. Bridenbaugh, "Parallel AC/DC transmission lines steady-state induction issues," *IEEE Trans. Power Del.*, vol. 4, no. 1, pp. 667–674, Jan. 1989.

[92] H. Ding, Y. Zhang, A. M. Gole, D. A. Woodford, M. X. Han, and X. N. Xiao, "Analysis of coupling effects on overhead VSC-HVDC transmission lines from AC lines with shared right of way," *IEEE Trans. Power Del.*, vol. 25, no. 4, pp. 2976–2986, Oct. 2010.

[93] R. S. Burton, C. F. Fuchshuber, D. A. Woodford, and A. M. Gole, "Prediction of core saturation instability at an HVDC converter," *IEEE Trans. Power Del.*, vol. 11, no. 4, pp. 1961–1969, Oct. 1996.

[94] S. Chen, A. R. Wood, and J. Arrillaga, "HVDC converter transformer core saturation instability: A frequency domain analysis," *IEE Proc. Gener. Transmiss. Distrib.*, vol. 143, no. 1, pp. 75–81, Jan. 1996.

[95] Y. Lin, Z. Xu, L. Xiao, Z. Zhang, and H. Xiao, "Analysis of coupling effect on LCC-MCC hybrid HVDC from parallel AC lines in close proximity," in *Proc. IEEE Power Energy Soc. Gen. Meeting*, Jul. 2015, pp. 1–5.

[96] X. N. Li, W. P. Jiang, T. Li, Z. H. Zeng, and Y. N. Wu, "Influence of AC transmission lines on parallelly erected UHVDC transmission lines and suppression measures," *Power Syst. Technol.-Beijing*, vol. 32, no. 11, pp. 1–6, 2008.

[97] T. Hasegawa, M. Hatano, K. Yamaji, T. Kouan, and N. Hosokawa, "Dielectric strength of transformer insulation at DC polarity reversal," *IEEE Trans. Power Del.*, vol. 12, no. 4, pp. 1526–1531, Oct. 1997.

[98] I. Ohshima, S. Motegi, M. Honda, T. Yanari, and Y. Ebisawa, "HVDC breakdown of transformer oil and the effect of space charge on it," *IEEE Trans. Power App. Syst.*, vol. PAS-102, no. 7, pp. 2208–2215, Jul. 1983.

[99] *Power Transformers—Insulation Levels, Dielectric Tests and External Clearances in Air*, Standard IEC 60076-3, Mar. 2018.

[100] M. Haueusler, H. Huang, and K. Papp, "Design and testing of 800 kV HVDC equipment," CIGRE, Paris, France, Tech. Rep., B4-115, 2008.

[101] U. Gafvert, A. Jaksts, C. Tornkvist, and L. Walfridsson, "Electrical field distribution in transformer oil," *IEEE Trans. Electr. Insul.*, vol. 27, no. 3, pp. 647–660, Jun. 1992.

[102] M. J. P. Jeroense and P. H. F. Morshuis, "Electric fields in HVDC paper-insulated cables," *IEEE Trans. Dielectr. Electr. Insul.*, vol. 5, no. 2, pp. 225–236, Apr. 1998.

[103] U. Piovan, "Insulation systems for HVDC transformers: Present configurations, trends, challenges, solutions and open points," in *Proc. IEEE Int. Conf. Solid Dielectr. (ICSD)*, Jun. 2013, pp. 254–257.

[104] S. Cho, Y. Lee, Y. Kim, and J. Koo, "DC field distribution in HVDC transformer considering the effects of space charge and temperature due to presence of oil immersed pressboard," *IEEE Trans. Dielectr. Electr. Insul.*, vol. 21, no. 2, pp. 866–872, Apr. 2014.

[105] R. Liu, A. Jaksts, C. Tornkvist, and M. Bergkvist, "Moisture and space charge in oil-impregnated pressboard under HVDC," in *Proc. IEEE 6th Int. Conf. Conduction Breakdown Solid Dielectr.*, Vasteras, Sweden, Jun. 1998, pp. 17–22.
[106] J. Beyer, P. H. F. Morshuis, and J. J. Smit, "Investigation on charging and polarization effects at dielectric interfaces in laminated HVDC insulation," in *Proc. Annu. Rep. Conf. Elect. Insul. Dielectr. Phenomena*, Oct. 1999, pp. 32–37.
[107] Y. Ebisawa, S. Yamada, S. Mori, and T. Teranishi, "DC creepage breakdown characteristics of oil-immersed insulation," *IEEE Trans. Dielectr. Electr. Insul.*, vol. 16, no. 6, pp. 1686–1692, Dec. 2009.
[108] L. Yang, S. M. Gubanski, Y. V. Serdyuk, and J. Schiessling, "Dielectric properties of transformer oils for HVDC applications," *IEEE Trans. Dielectr. Electr. Insul.*, vol. 19, no. 6, pp. 1926–1933, Dec. 2012.
[109] F. K. Padgham, W. G. Lawson, and P. Metra, "The effect of polarity reversals on the dielectric strength of oil-impregnated paper insulation for H.V.D.C. Cables," *IEEE Trans. Power App. Syst.*, vol. PAS-97, no. 3, pp. 884–892, May 1978.
[110] T. T. N. Vu, G. Teyssedre, B. Vissouvanadin, S. L. Roy, and C. Laurent, "Correlating conductivity and space charge measurements in multi-dielectrics under various electrical and thermal stresses," *IEEE Trans. Dielectr. Electr. Insul.*, vol. 22, no. 1, pp. 117–127, Feb. 2015.
[111] W. Sun, L. Yang, F. Zare, Y. Xia, L. Cheng, and K. Zhou, "3D modeling of an HVDC converter transformer and its application on the electrical field of windings subject to voltage harmonics," *Int. J. Electr. Power Energy Syst.*, vol. 117, pp. 1–10, May 2020, Art. no. 105581.
[112] M. A. Fard, A. J. Reid, and D. M. Hepburn, "Analysis of HVDC superimposed harmonic voltage effects on partial discharge behavior in solid dielectric media," *IEEE Trans. Dielectr. Electr. Insul.*, vol. 24, no. 1, pp. 7–16, Feb. 2017.
[113] M. A. Fard, A. J. Reid, D. M. Hepburn, and H. Gallagher, "Influence of voltage harmonic phenomena on partial discharge behavior at HVDC," in *Proc. IEEE Int. Conf. Dielectr. (ICD)*, vol. 1, Jul. 2016, pp. 548–551.
[114] G. Liu, L. Li, F. Ji, and Y. Sun, "Quasi-static electric field computation of converter transformer by adaptive time step FEM," in *Proc. Int. Conf. Comput. Problem-Solving*, Dec. 2010, pp. 157–160.
[115] Z. Liang-Xian, Z. Qi-Min, C. Mo-Sheng, and P. Zong-Ren, "Research on transient electric field distribution of converter transformer valve side winding under polarity reversal," in *Proc. Annu. Rep. Conf. Elect. Insul. Dielectr. Phenomena*, Oct. 2013, pp. 307–310.
[116] Z.-H. Pu, J.-J. Ruan, Z.-Y. Du, Y.-D. Zhang, J.-L. Li, Q.-J. Xie, and D. Tan, "Analysis of voltage distribution characteristics in UHVDC converter transformer winding based on the reduced-scale model," *IEEE Trans. Magn.*, vol. 50, no. 11, pp. 1–5, Nov. 2014.
[117] M. Yea, K. J. Han, J. Park, S. Lee, and J. Choi, "Design optimization for the insulation of HVDC converter transformers under composite electric stresses," *IEEE Trans. Dielectr. Electr. Insul.*, vol. 25, no. 1, pp. 253–262, Feb. 2018.
[118] L. Yuncai and L. Wei, "Study on condition assessment and fault diagnosis for converter transformers," in *Proc. IEEE Int. Conf. High Voltage Eng. Appl. (ICHVE)*, Sep. 2016, pp. 1–4.
[119] F. Wang, T.-Q. Liu, and X.-Y. Li, "Decreasing the frequency of HVDC commutation failures caused by harmonics," *IET Power Electron.*, vol. 10, no. 2, pp. 215–221, Apr. 2016.
[120] G. M. Bastos, J. C. Brandao, J. Santelli, R. Albuquerque, S. Arenare, J. C. Mendes, and J. Hajek, "HVDC converter transformer performance on Itaipu system," CIGRE Paris, France, Tech. Rep., B4-201, 2006.

MARCOS V. CZERNORUCKI was born in São Paulo, Brazil, in 1975. He received the B.Sc. and M.Sc. degrees from the University of São Paulo (USP), in 2001 and 2008, respectively, where he is currently pursuing the Ph.D. degree in electrical engineering with the Polytechnic School. His research interests include the different types of transformers, such as industrial, phase-shifters, and converter transformers, their interaction with the power systems, under a design prospective. He is a member of Cigré Brazil, participating actively on the working group A2.09 and on standards revision for ABNT, the Brazilian Technical Standard Association.

MAURICIO B. C. SALLES (Member, IEEE) received the M.Sc. degree from the State University of Campinas (UNICAMP), São Paulo, Brazil, in 2004, and the Ph.D. degree from the University of São Paulo (USP), São Paulo, in 2009. From 2006 to 2008, he was the research team of the Institute of Electrical Machines, RWTH Aachen University. From 2014 and 2015, he was a Visiting Scholar at the Harvard John A. Paulson School of Engineering and Applied Sciences. He has been an Assistant Professor with the Laboratory of Advanced Electric Grids, Polytechnic School, USP, since 2010. His main research interests include distributed generation, power system dynamics, control and stability, renewable energy, energy storage, and electricity markets.

EDUARDO C. M. COSTA (Member, IEEE) received the Ph.D. degree in electrical engineering from the University of Campinas (Unicamp), São Paulo, Brazil, in 2013. He is has been an Assistant Professor at the Polytechnic School, University of São Paulo, since 2015. His research interests include HVAC/HVDC power transmission systems, electromagnetic transients, power system modeling, measurements, and identification methods applied to parameters estimation of power systems.

ANDRE S. MELO received the B.Sc. and M.Sc. degrees in electrical engineering from the Faculty of Engineering, University of São Paulo, Brazil, in 2011 and 2017, respectively, where he is currently pursuing the Ph.D. degree in electrical engineering with the Polytechnic School. His research interests include power transformer insulation and internal design, power systems modeling, electromagnetic transients on power systems, high-voltage techniques for experimental analyses, and insulation coordination.

LUIGI PIEGARI (Senior Member, IEEE) was born in 1975. He received the M.S. and Ph.D. degrees in electrical engineering from the University of Naples Federico II, Naples, Italy, in 1999 and 2003, respectively. He is currently an Associate Professor of electrical machine, drives and power electronics at the Department of Electronics, Information and Bioengineering, (DEIB), Politecnico di Milano, Milan, Italy. His current research interests include electrical machines, high efficiency power electronic converters, dc distribution grids, renewable energy sources, and storage systems modeling.